Pt Nanoparticles Anchored on NH₂-MIL-101 with Efficient Peroxidase-Like Activity for Colorimetric Detection of Dopamine

Jing Li [1,†], Keying Xu [1,†], Yang Chen [1], Jie Zhao [1], Peiyao Du [1], Libing Zhang [1], Zhen Zhang [1,*] and Xiaoquan Lu [2,*]

[1] Tianjin Key Laboratory of Molecular Optoelectronic, Department of Chemistry, School of Science, Tianjin University, Tianjin 30072, China; 18856162507@163.com (J.L.); xukeying@tju.edu.cn (K.X.); 18810551270@163.com (Y.C.); zhaojie_2018@163.com (J.Z.); peiyao.du@tju.edu.cn (P.D.); libing.zhang@tju.edu.cn (L.Z.)

[2] Key Laboratory of Bioelectrochemistry and Environmental Analysis of Gansu Province, College of Chemistry and Chemical Engineering, Northwest Normal University, Lanzhou 730070, China

* Correspondence: zhzhen@tju.edu.cn (Z.Z.); luxq@tju.edu.cn or luxq@nwnu.edu.cn (X.L.)

† These authors contributed equally to this work.

1. Experimental Section

1.1 Materials

N,N-Dimethylformamide (DMF), acetone, dopamine (DA), urea, uric acid, histidine, lysine, tryptophan, alanine, serine, tyrosine, 2-aminotereph-thalic acid (NH₂-BDC), sodium hydrogen phosphate dihydrate, hexane, sodium dihydrogen phosphate anhydrous were purchased from Sun Chemical Technology (Shanghai) Co., Ltd. Terephthalic (TA), H₂PtCl₆·6H₂O, Polyvinyl pyrrolidone (PVP, Mw=58 000), FeCl₃·6H₂O, CH₃COOH, CH₃COONa, ethylene glycol, 1, 2-diaminobenzene (OPD), hydrogen peroxide (H₂O₂, 30%), 2, 2'-azino-bis(3-ethylbenzothiazoline-6-sulfonic acid) (ABTS) were all purchased from Shanghai Aladdin Biochemical Technology Co., Ltd. 3, 3', 5, 5'-tetramethylbenzidine (TMB) was obtained from Shanghai Adamas Reagent Co., Ltd. Ultrapure water (≥18 MΩ, Millipore) was used in all experiments

1.2 Instruments

The scanning electron microscopy (SEM) images were performed using a Hitachi SU8010 (Hitachi, Tokyo, Japan) scanning electron microscope. The transmission electron microscope (TEM) images, The high-resolution TEM (HRTEM), and elemental mapping analyses were conducted on a JEOL-2100F (JEOL, Tokyo, Japan). Powder X-ray diffraction (XRD) patterns were obtained from a Rigaku Smart Lab (Rigaku Corporation, Tokyo, Japan). A Thermo Fisher K-alpha X-ray photoelectron spectrometer using a monochromatic Al Kα radiation excitation source was used to measure X-ray photoelectron spectra (XPS) (Thermo Fisher, Massachusetts, USA). The Fourier transform Infrared (FT-IR) spectra were characterized by a Nicolet FT-170SX spectrometer within 500–4000 cm⁻¹ (Thermo Fisher, Massachusetts, USA). The amount of Pt NPs in NH₂-MIL-101 was measured by an inductively coupled plasma source mass spectrometer (ICP-MS) (Agilent, California, USA). The Brunauer-Emmett-Teller (BET) surface area of the samples was obtained with Anton Paar Autosorb-IQ analyzer (Anton Paar, Florida, USA). Fluorescence spectra were obtained using an FS5 fluorescence spectrometer (Thermo Fisher, Edinburgh, United Kingdom). All the Ultraviolet-visible (UV-vis) absorbance spectra were measured by UV756CRT (YOKE Instrument, ShangHai, China).

1.3 Synthesis of NH₂-MIL-101

NH₂-MIL-101 was synthesized with minor modifications based on previous reports [1]. 36.2 mg NH₂-BDC (0.2 mmol) and 108.0 mg FeCl₃·6H₂O (0.4 mmol) were added to 20 mL DMF solution. The solution was completely dissolved by ultrasonic treatment at room temperature and then stirred for 1 h. The mixture was then transferred to a 30 mL

Teflon autoclave and reacted in an oven at 110 °C for 24 h. After the reaction, the sample was naturally cooled to room temperature, the precipitate was separated from the reaction mixture by centrifugation (1000 rpm, 10 min), and the unreacted feedstock was washed several times with DMF and ethanol to remove. Then, the precipitate was immersed in ethanol for 24 h to achieve the exchange of guest solvent molecules with ethanol, and collected by centrifugation. Finally, the obtained brown solid was vacuum dried at 60°C for 12 h for further characterization and modification.

1.4 Synthesis of Pt NPs

The synthesis of Pt NPs was slightly modified according to the reported [2], and the specific operations were as follows: First, PVP (222 mg, Mw = 58,000) was completely dissolved in 20 mL ethylene glycol solution under ultrasound, and then 50.75 mg $H_2PtCl_6·6H_2O$ was added to the solution until the solution was dissolved by ultrasound. The mixed solution was then transferred to a 50 mL round-bottomed flask for 10 min in an oil bath at 180 °C. After cooling to room temperature, the obtained dark brown solution was added to 120 mL acetone and centrifuged at 10,000 rpm for 10 min to obtain PVP-coated Pt NPs. Finally, the precipitate was washed several times with acetone-hexane (v/v= 1:1) to remove excess PVP, and the Pt NPs were dispersed in 20 mL DMF for later use.

1.5 Determined the catalytic ability of NH₂-MIL-101, Pt NPs, and Pt/NH₂-MIL-101

The specific operation is as follows: 50 μL Pt NPs (2.5 μg/mL), NH₂-MIL-101 (1 mg/mL) and Pt/NH₂-MIL-101 (1 mg/mL) were added into three equal volumes of HAc-NaAc buffer solution (0.1 M pH = 4.0), respectively. Then 50 μL TMB (10 mM) and 50 μL H_2O_2 (10 mM) were added into the mixture and reacted for 10 min. The absorbance of the reaction system at 652 nm was determined to evaluate the catalytic ability of each material.

1.6 Evaluate the effect of reaction conditions on the peroxidase-like activity of Pt/NH₂-MIL-101

1.6.1 Optimize pH

The mixed solution of 50 μL Pt/NH₂-MIL-101 (800 μg/mL), 50 μL TMB (10 mM) and 50 μL H_2O_2 (10 mM) was added into 1850 μL HAc-NaAc (0.1 M) buffer solution with pH 3.0–9.0, respectively. After reacting at 25 °C for 10 min, recorded the UV absorbance values at 652 nm at different pH values, and measured them three times to reduce the experimental error.

1.6.2 Optimizing temperature

The mixed solution of 50 μL Pt/NH₂-MIL-10 (800 μg/mL), 50 μL TMB (10 mM) and 50 μL H_2O_2 (10 mM) was added into 1850 μL HAc-NaAc (0.1 M, pH=4.0) buffer solution, respectively. The mixed solution was reacted at a constant temperature of 25–70 °C for 10 minutes, and three groups of data were still measured to observe the change in absorbance with temperature and measured three times to reduce the experimental error.

1.6.3 Steady state dynamic analysis

The catalytic activity of the Pt/NH₂-MIL-101 hybrid nanozyme was mainly evaluated by the Michaelis-Menten equation and double reciprocal linear fitting curve. Kinetic parameters v_{max}, k_m were mainly calculated by Michaelis-Menten and Lineweaver-Burk equations:

$$v = \frac{v_{max}\,[s]}{k_m + [s]} \qquad (1)$$

$$\frac{1}{v} = \frac{k_m}{v_{max}} \bullet \frac{1}{s} + \frac{1}{v_{max}} \qquad (2)$$

Where v was the initial speed, v_{max} was the maximum reaction rate, k_m was the Michaelis-Menten constant, and $[s]$ was the concentration of the substrate TMB or H_2O_2.

The specific experimental operations were as follows:

200 µL TMB (0.25–7.0 mM) was added as substrate in 1650 µL HAc-NaAc buffer solution (0.1 M, pH = 4.0) mix with 50 µL 800 µg/mL Pt/NH$_2$-MIL-101 and 100 µL H_2O_2 (10 mM), or 200 µL H_2O_2 (2.0–14.0 mM) as a substrate, mixed with 50 µL 800 µg/mL Pt/NH$_2$-MIL-101 and 100 µL TMB (10 mM), and added into 1650 µL HAc-NaAc buffer solution. The absorbance change curves of each reaction at 652 nm under different time conditions were recorded using a UV-vis spectrometer at room temperature.

1.7 Selective Experiments

In the selective experiment of DA detection, K^+, Na^+, Ca^{2+}, histidine, lysine, tryptophan, urea, and other ions or amino acids in the human body with an initial concentration of 6 mM were selected as interferers substances to replace DA in the above steps, and their selectivity was determined. The concentration of the interfering substance was 10 times that of DA. Each experiment was performed three times to minimize error.
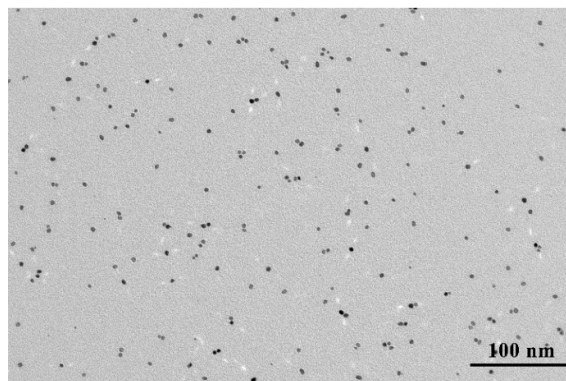
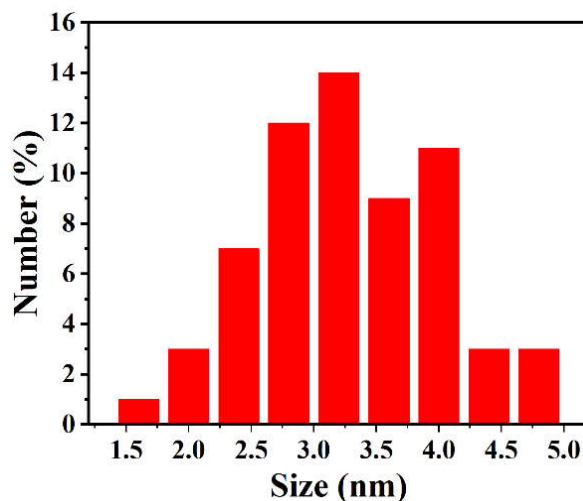

Figure S1. TEM image of Pt NPs**.**
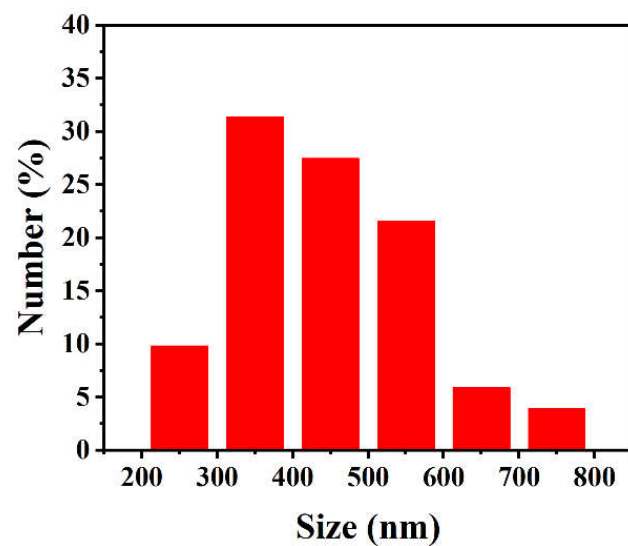

Figure S2. Particle size distribution of Pt NPs.

Figure S3. The particle size distribution of Pt/NH₂-MIL-101.

Figure S4. XPS spectrum of Pt/NH₂-MIL-101.
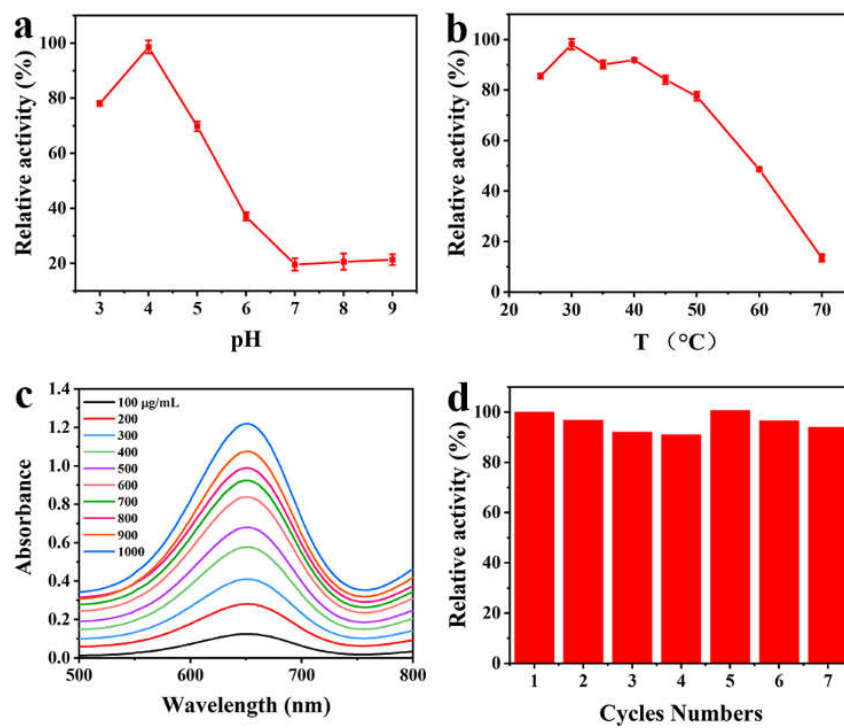
Figure S5. (**a**) pH. (**b**) Temperature. (**c**) The concentration of Pt/NH$_2$-MIL-101. (**d**) The effect of cycles on the peroxidase-like activity of Pt/NH$_2$-MIL-101.

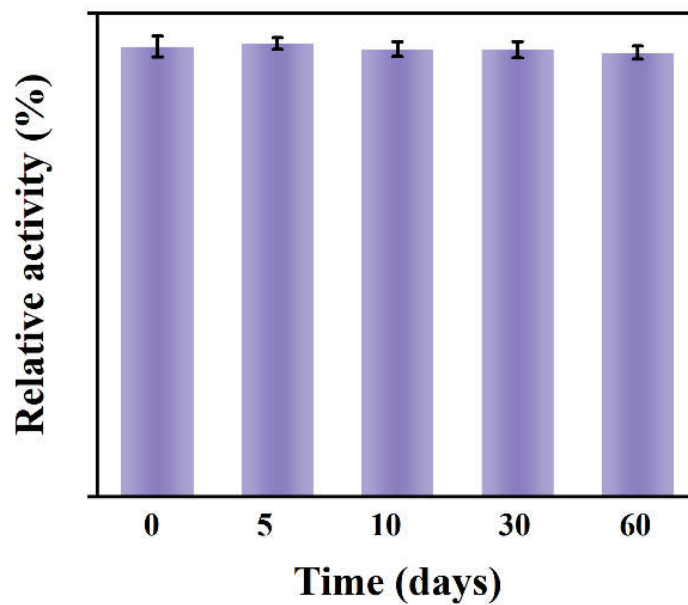**Figure S6.** The stability of the Pt/NH$_2$-MIL-101.

Table S1. Elements content of Fe and Pt in Pt/NH$_2$-MIL-101.

Sample	Fe (wt%)	Pt (wt%)
Pt/NH$_2$-MIL-101	4.25	4.59

Table S2. Compare the k_m and v_{max} between Pt/NH$_2$-MIL-101 and other nanozymes.

Catalyst	Substrate	v_{max} (M S^{-1})	k_m (mM)	Reference
HRP	TMB	1.00×10^{-7}	0.43	
HRP	H$_2$O$_2$	8.71×10^{-8}	3.70	[3]
GOD@Cu-hemin MOF	TMB	7.12×10^{-8}	0.43	
GOD@Cu-hemin MOF	H$_2$O$_2$	4.19×10^{-8}	1.30	[4]
h-CuS NCs	TMB	1.66×10^{-7}	1.62	
h-CuS NCs	H$_2$O$_2$	2.55×10^{-8}	0.94	[5]
2.6Pt/EMT	TMB	4.72×10^{-8}	0.16	
2.6Pt/EMT	H$_2$O$_2$	4.72×10^{-8}	0.58	[6]
BNQDs/CeO$_2$@Apt	TMB	0.87×10^{-8}	0.19	
BNQDs/CeO$_2$@Apt	H$_2$O$_2$	1.02×10^{-7}	4.53	[7]
CeO$_2$ Rod	TMB	2.743×10^{-9}	0.230	
CeO$_2$ Rod	H$_2$O$_2$	4.302×10^{-8}	302	[8]
Fe-MOF	TMB	5.6×10^{-8}	0.026	
Fe-MOF	H$_2$O$_2$	2.5×10^{-8}	0.013	[9]
Pt/CoSn(OH)$_6$	TMB	6.84×10^{-8}	0.12	[10]
Pt/CoSn(OH)$_6$	H$_2$O$_2$	1.21×10^{-8}	0.02	
Pt/NH$_2$-MIL-101	TMB	1.15×10^{-7}	0.12	**This work**
Pt/NH$_2$-MIL-101	H$_2$O$_2$	1.97×10^{-7}	0.48	

Table S3. Comparison analytical performance of the Pt/NH$_2$-MIL-101 with that of other reported nanomaterials for dopamine detection.

Material	Linear range (M)	LOD (M)	Reference
Nf-Ag@HCS/GC	20–70	0.6	[11]
RGO-ZnO/GCE	3–33	1.08	[12]
Cu(PDA)(DMF)	10–100	-	[13]
Co$_3$O$_4$@NiO	1–20	1.2	[14]
Pt/hBBNS	2–50	0.76	[15]
Cu^{2+}	1–50	1.0	[16]
CMCNs	1–10	0.17	[17]
AuNRs-IO$_3^-$	0.8–60	0.62	[18]
WS$_2$ QDs	3–50	3.3	[19]
CoFe$_2$O$_4$/CoS	0–50	0.58	[20]
Pt/NH$_2$-MIL-101	1–60	0.42	**This work**

References

[1] Dao, X.; Xie, X.; Guo, J.; Zhang, X.; Kang, Y.; Sun, W. Boosting photocatalytic CO$_2$ reduction efficiency by heterostructures of NH$_2$-MIL-101(Fe)/g-C$_3$N$_4$. *ACS Appl. Energy Mater*. **2020**, *3*, 3946–3954.

[2] Liu, C.; Xing, J.; Akakuru, O. U.; Luo, J.; Sun, S.; Zou, R.; Yu, Z.; Fang, Q.; Wu, A. Nanozymes-engineered metal-organic frameworks for catalytic cascades-enhanced synergistic cancer therapy. *Nano Lett*. **2019**, *19*, 5674–5682.

[3] Gao, L.; Zhuang, J.; Nie, L.; Zhang, J.; Zhang, Y.; Gu, N.; Wang, T.; Feng, J.; Yang, D.; Perrett, S.; Yan, X. Intrinsic peroxidase-like activity of ferromagnetic nanoparticles. *Nat. Nanotechnol*. **2007**, *2*, 577–583.

[4] Lin, C.; Du, Y.; Wang, S.; Wang, L.; Song, Y. Glucose oxidase@Cu-hemin metal-organic framework for colorimetric analysis of glucose. *Mater. Sci. Eng. C*. **2021**, *118*, 111511.

[5] Zhu, J.; Peng, X.; Nie, W.; Wang, Y.; Gao, J.; Wen, W.; Selvaraj, J.; Zhang, X.; Wang, S. Hollow copper sulfide nanocubes as multifunctional nanozymes for colorimetric detection of dopamine and electrochemical detection of glucose. *Biosens. Bioelectron*. **2019**, *141*, 111450.

[6] Li, X.; Yang, X.; Cheng, X.; Zhao, Y.; Luo, W.; Elzatahry, A.; Alghamdi, A.; He, X.; Su, J.; Deng, Y. Highly dispersed Pt nanoparticles on ultrasmall EMT zeolite: A peroxidase-mimic nanoenzyme for detection of H$_2$O$_2$ or glucose. *J. Colloid Interface Sci*. **2020**, *570*, 300–311.

[7] Zhu, X.; Tang, L.; Wang, J.; Peng, B.; Ouyang, X.; Tan, J.; Yun, J.; Feng, H.; Tang, J. Enhanced peroxidase-like activity of boron nitride quantum dots anchored porous CeO_2 nanorods by aptamer for highly sensitive colorimetric detection of kanamycin. *Sens. Actuators B Chem*. **2020**, *330*, 129318.

[8] Zhang, J.; Tan, Z.; Leng, W.; Chen, Y.; Zhang, S.; Lo, B.; Yung, K.; Peng, Y. Chemical state tuning of surface Ce species on pristine CeO_2 with 2400% boosting in peroxidase-like activity for glucose detection. *Chem. Commun*. **2020**, *56*, 7897–7900.

[9] Xu, W.; Jiao, L.; Yan, H.; Wu, Y.; Chen, L.; Gu, W.; Du, D.; Lin, Y.; Zhu, C. Glucose oxidase-integrated metal-organic framework hybrids as biomimetic cascade nanozymes for ultrasensitive glucose biosensing. *ACS Appl. Mater. Interfaces* **2019**, *11*, 22096–22101.

[10] Georgi, A.; Velasco, M.; Crincoli, K.; Mackenzie, K.; Kopinke, F. Accelerated catalytic fenton reaction with traces of iron: An Fe-Pd-multicatalysis approach. *Environ. Sci. Technol*. **2016**, *50*, 5882–5891.

[11] Zhang, X.; Zhang, J. Hollow carbon sphere supported Ag nanoparticles for promoting electrocatalytic performance of dopamine sensing. *Sens. Actuators B Chem*. **2019**, *290*, 648–655.

[12] Zhang, X.; Zhang, Y.; Ma, L. One-pot facile fabrication of graphene-zinc oxide composite and its enhanced sensitivity for simultaneous electrochemical detection of ascorbic acid, dopamine and uric acid. *Sens. Actuators B Chem*. **2016**, *227*, 488–496.

[13] Zhu, Y.; Yang, Z.; Chi, M.; Li, M.; Wang, C.; Lu, X. Synthesis of hierarchical Co_3O_4@NiO core-shell nanotubes with a synergistic catalytic activity for peroxidase mimicking and colorimetric detection of dopamine. *Talanta*. **2018**, *181*, 431–439.

[14] Ivanova, M. N.; Grayfer E. D.; Plotnikova, E. E.; Kibis, L. S.; Darabdhara, D.; Boruah, P. K.; Das, M. R.; Fedorov, V. E. Pt-decorated boron nitride nanosheets as artificial nanozyme for detection of dopamine. *ACS Appl. Mater. Interfaces* **2019**, *11*, 22102–22112.

[15] Wang, H.; Li, Y.; Dong, G.; Gan, T.; Liu, Y. A convenient and label-free colorimetric assay for dopamine detection based on the inhibition of the Cu(II)-catalyzed oxidation of a 3, 3', 5, 5'-tetramethylbenzidine-H_2O_2 system. *New J. Chem*. **2017**, *41*, 14364–14369.

[16] Wang, J.; Hu, Y.; Zhou, Q.; Hu, L.; Fu, W.; Wang, Y. Peroxidase-like activity of metal-organic framework [Cu(PDA)(DMF)] and its application for colorimetric detection of dopamine. *ACS Appl. Mater. Interfaces* **2019**, *11*, 44466–44473.

[17] Gajendar, S.; Amisha, K.; Manu. S. Mildly acidic pH and room temperature triggered peroxidase-mimics of rGO-$Cu_3(OH)_2(MoO_4)_2$ cuboidal nanostructures: an effective colorimetric detection of neurotransmitter dopamine in blood serum and urine samples. *CrystEngComm*. **2021**, *23*, 599–616.

[18] Qin, X.; Yuan, C.; Shi, R.; Wang, S.; Wang, Y. Colorimetric detection of dopamine based on iodine-mediated etching of gold nanorods. *Chin. J. Anal. Chem.*, **2021**, *49*, 60–67.

[19] Zhao, X.; He, D.; Wang, Y.; Fu, C. Facile fabrication of tungsten disulfide quantum dots (WS_2 QDs) as effective probes for fluorescence detection of dopamine (DA). *Mater. Chem. Phys*. **2018**, *207*, 130–134.

[20] Yang, Z.; Zhu, Y.; Chi, M.; Wang, C.; Wei, Y.; Lu, X. Fabrication of cobalt ferrite/cobalt sulfide hybrid nanotubes with enhanced peroxidase-like activity for colorimetric detection of dopamine. *J. Colloid Interface Sci*. **2018**, *511*, 383–391.